The numerical treatment of singular integrals in boundary element calculations

C.J. Huber, W. Rieger, M. Haas and W.M. Rucker
Institut für Theorie der Elektrotechnik, Universität Stuttgart,
Pfaffenwaldring 47, D-70569 Stuttgart, Germany

Abstract **- In this paper a general method for the evaluation of singular boundary element integrals over three-dimensional isoparametric boundary elements of higher order is presented. This method permits an efficient integration of strongly singular kernels of order $O(1/r^2)$ and of nearly strong singular kernels on curved surfaces. For numerical examples the proposed integration scheme is compared with analytical test examples showing high efficiency and accuracy. This new method has full generality and, therefore, can be applied in any field of electromagnetics. The actual computation can be easily included in any existing computer code, e. g. for the solution of electromagnetic scattering problems.**

I. INTRODUCTION

Many boundary integral equations in three-dimensional space contain, at least a weak singularity (integrable across the singularity in the sense of an ordinary improper integral) or a strong singularity (not integrable in the improper sense), usually both. Some integral equations of electromagnetics contain in addition even hypersingular integrals. The hypersingular integrals can be avoided in one of two ways:

The first is to use integration by parts to improve the singularity of the kernels at the expense of differentiation of the density or boundary variable function. This results in a strongly singular integral with the unknown being the surface divergence of the density function. Most of these methods are based on either the electric- and magnetic-field integral equations (EFIE) and (MFIE) or the combined field integral equation (CFIE) [1]-[4].

The second way is to transform analytically this surface divergence term into the normal component of the fields. This results in more unknowns to be solved and also a strongly singular kernel function [9].

Consequently, one of the key problems of integral methods is the integration of strongly and weakly singular kernels in which higher order shape functions represent the local behavior of the unknown function. Nearly singular integrals or nearly strong singular integrals will occur in applications of BEM whenever the observation point is close to the surface on which the integrations have to be performed.

In many cases it is too complicated or even impossible to integrate analytically higher order element types. The natural and most common numerical practice in BEM applications is to use more integration (Gaussian) points on the surface which is usually subdivided into small cells to ensure convergence. This simple approach certainly works but at a very high price. The computer time consumed by evaluations of these singular integrals in this way is, in most cases, many times longer than that used by evaluations of other integrals. Many methods have been devised to deal with surface integrals defined in the Cauchy principal value sense. They have the common feature of avoiding the direct computation of strongly singular integrals by employing known elementary solutions of the boundary integral equation. But these indirect approaches fail if solutions of the boundary integral equations are not available [6].

One of the aims of the present paper is to show that the difficulty in directly computing any type of Cauchy principal value and nearly singular integrals arising in BEM is only apparent. It will be demonstrated that Cauchy principal value integrals defined on curved surface elements can be always transformed in ordinary integrals through rigorous manipulations.

The boundary element method formulation applied here uses eight-noded quadrilateral isoparametric surface elements shown in Fig. 1a and point collocation is used to provide a set of equations for the solution.

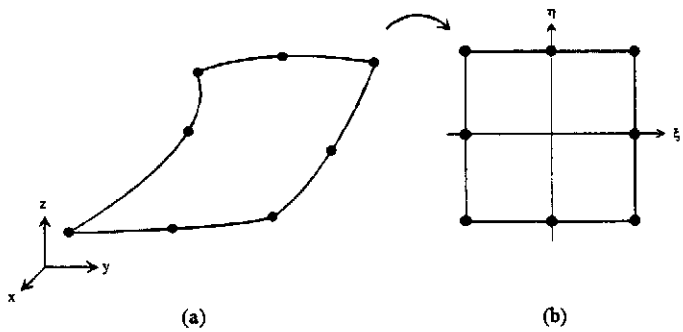

Fig. 1. Eight- noded surface element in the global coordinate system and in the local parameter space.

Subdomain expansion by shape functions is used to link each element in global space where ξ and η are the intrinsic coordinates (see Fig. 1). The global coordinates and the unknown functions are then defined in terms of their interpolation values.

II. REGULARIZATION OF CAUCHY PRINCIPAL VALUE INTEGRALS

Regularization [5], [6] here refers to singularity cancellation by subtraction of successive terms of a Taylor expansion of the singular kernel function. It is a technique used to isolate strongly singular integrals from the numerically calculated integrand. The added back terms

Manuscript received September 23, 1996.
C. J. Huber, e-mail christian.huber@ite.uni-stuttgart.de, fax +49 711 685 7222

contain, of course, the same order singularities as the original, but these terms can be easy transformed in regular one-dimensional integrals around the singularity.

BEM integrals with strongly singular kernels occur when the kernel contains the gradient of a Green's function of the order O(1/r). In the following a strongly singular kernel function is considered as appeared in three-dimensional electromagnetic wave scattering problems

$$T(\mathbf{r},\mathbf{r}') = \frac{(\mathbf{r}-\mathbf{r}')\cdot\mathbf{u}}{|\mathbf{r}-\mathbf{r}'|^3}. \tag{1}$$

Other strongly singular kernel functions can be treated similarly. The term $|\mathbf{r}-\mathbf{r}'|$ represents the distance between the source point $\mathbf{r}'$ and the observation point $\mathbf{r}$, and $\mathbf{u}$ is the global unit normal vector at the observation point. For such a kernel of order $O(1/r^2)$ the boundary element integral (2) only exists in the Cauchy principal value sense

$$I = \sum_m \iint_{Sm} T(\mathbf{r},\mathbf{r}'(\xi,\eta))\, N(\xi,\eta) J(\xi,\eta) d\xi\, d\eta, \tag{2}$$

where $N(\xi,\eta)$ represents the shape function and $J(\xi,\eta)$ is the Jacobian. Obviously, all m elements neighboring the pole must be considered, since at the limit any single contribution is unbounded. It is convenient to introduce in each element neighboring the pole a polar coordinate system (ρ, φ) centered at the local coordinate (ξ_1, η_1) of the singular point $\mathbf{r}$. (see Fig. 2b)

$$\begin{aligned} \xi &= \xi_1 + \rho\cos\varphi \\ \eta &= \eta_1 + \rho\sin\varphi \end{aligned} \tag{3}$$

Now the new integrand in polar coordinates

$$F(\rho,\varphi) = T(\mathbf{r},\mathbf{r}'(\xi,\eta))\, N(\xi,\eta) J(\xi,\eta)\, \rho \tag{4}$$

becomes singular of order O(1/r), because ρ cancels out one order of the singular kernel function. In the neighborhood of the singularity $|\mathbf{r}-\mathbf{r}'|$ is expanded into a Taylor series as

$$\begin{aligned} \mathbf{r}-\mathbf{r}' &= \left.\frac{\partial \mathbf{r}'(\xi,\eta)}{\partial\xi}\right|_{\xi_1,\eta_1}(\xi_1-\xi) + \left.\frac{\partial \mathbf{r}'(\xi,\eta)}{\partial\eta}\right|_{\xi_1,\eta_1}(\eta_1-\eta) + O(\rho^2) \\ &= \rho\left[-\left.\frac{\partial \mathbf{r}'(\xi,\eta)}{\partial\xi}\right|_{\xi_1,\eta_1}\cos\varphi - \left.\frac{\partial \mathbf{r}'(\xi,\eta)}{\partial\eta}\right|_{\xi_1,\eta_1}\sin\varphi\right] + O(\rho^2) \end{aligned} \tag{5}$$

where ρ is the intrinsic distance

$$\rho^2 = (\xi_1-\xi)^2 + (\eta_1-\eta)^2 \tag{6}$$

and

$$\mathbf{A}(\varphi) = -\left.\frac{\partial \mathbf{r}'(\xi,\eta)}{\partial\xi}\right|_{\xi_1,\eta_1}\cos\varphi - \left.\frac{\partial \mathbf{r}'(\xi,\eta)}{\partial\eta}\right|_{\xi_1,\eta_1}\sin\varphi, \tag{7}$$

$$A(\varphi) = \sqrt{A_1(\varphi)^2 + A_2(\varphi)^2 + A_3(\varphi)^2}. \tag{8}$$

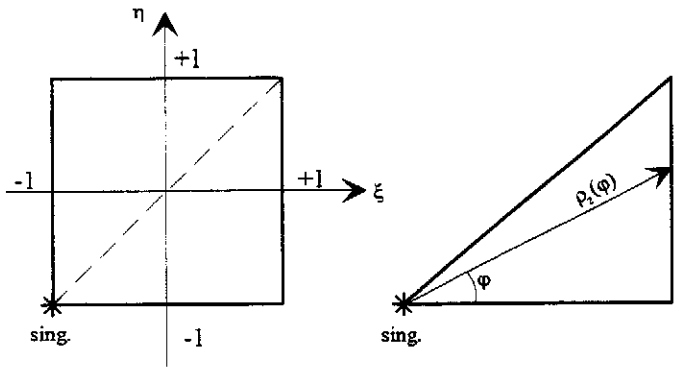

Fig. 2. Subdivision of a rectangular element into two triangles if the observation point lies in a corner node (a) using polar coordinates in the local parameter plane (b).

Equation (5) can be written as

$$\mathbf{r}-\mathbf{r}' = \rho\,\mathbf{A}(\varphi) + 0(\rho^2). \tag{9}$$

Using (8) and (9) the following equation is easily obtained

$$\frac{\mathbf{r}-\mathbf{r}'}{|\mathbf{r}-\mathbf{r}'|} = \frac{\mathbf{A}(\varphi)}{A(\varphi)} + 0(\rho). \tag{10}$$

It is now possible to give explicitly the asymptotic expression of the singular integrand function (4)

$$\begin{aligned} F(\rho,\varphi) &= \frac{1}{\rho}\left[\frac{\mathbf{u}\cdot\mathbf{A}(\varphi)}{A(\varphi)^3} N(\xi_1,\eta_1) J(\xi_1,\eta_1) + O(\rho)\right] \\ &= \frac{1}{\rho}\left[f(\varphi) + O(\rho)\right]. \end{aligned} \tag{11}$$

It is important to note, that in (11) the Jacobian and the local shape functions are calculated at the singular point (ξ_1, η_1) only. From (11) immediately follows that

$$\left|F(\rho,\varphi) - \frac{f(\varphi)}{\rho}\right| \le |k| \qquad \text{if} \qquad \rho \to 0 \tag{12}$$

is limited by $|k| < \infty$ if ρ tends to zero. Adding and subtracting the first term of the series expansion (11) in (2), we obtain

$$I = \lim_{\rho_0(\varphi)\to 0} \sum_m \int_{\varphi_{1m}}^{\varphi_{2m}} \int_{\rho_0(\varphi)}^{\rho_2(\varphi)} F(\rho,\varphi)\, d\rho\, d\varphi \tag{13}$$

and

$$I=\sum_{m}\int_{\varphi_{1m}}^{\varphi_{2m}}\int_{0}^{\rho_2(\varphi)}(F(\rho,\varphi)-f(\varphi)/\rho)\,d\rho\,d\varphi\;+$$

$$+\lim_{\rho_0(\varphi)\to 0}\sum_{m}\int_{\varphi_{1m}}^{\varphi_{2m}}\int_{\rho_0(\varphi)}^{\rho_2(\varphi)}f(\varphi)/\rho\;d\rho\,d\varphi\,. \tag{14}$$

The contour ρ_0 of the vanishing neighborhood

$$\varepsilon^2=(\mathbf{r}-\mathbf{r}')\cdot(\mathbf{r}-\mathbf{r}')=\rho^2A(\varphi)^2+O(\rho^3) \tag{15}$$

can be written now (first term of series expansion)

$$\rho_0(\varphi)=\frac{\varepsilon}{A(\varphi)}. \tag{16}$$

The added-back term in (14) can be transformed using (16)

$$\lim_{\rho_0(\varphi)\to 0}\sum_{m}\int_{\varphi_{1m}}^{\varphi_{2m}}\int_{\rho_0(\varphi)}^{\rho_2(\varphi)}f(\varphi)/\rho\;d\rho\,d\varphi=$$

$$=\sum_{m}\int_{\varphi_{1m}}^{\varphi_{2m}}f(\varphi)\ln\left[\rho_2(\varphi)A(\varphi)\right]d\varphi+\lim_{\varepsilon\to 0}\left[\ln(\varepsilon)\sum_{m}\int_{\varphi_{1m}}^{\varphi_{2m}}f(\varphi)d\varphi\right]. \tag{17}$$

The second integral on the right-hand side of (17) is vanishing. After these manipulations the final formula for the calculation of strongly singular integrals can be obtained

$$I=\sum_{m}\int_{\varphi_{1m}}^{\varphi_{2m}}\int_{0}^{\rho_2(\varphi)}(F(\rho,\varphi)-f(\varphi)/\rho)\,d\rho\,d\varphi\;+$$

$$+\sum_{m}\int_{\varphi_{1m}}^{\varphi_{2m}}f(\varphi)\ln\left[\rho_2(\varphi)A(\varphi)\right]d\varphi\,. \tag{18}$$

In (18) it can be seen that the first integral became a regular integral in the local polar coordinate system. The second integral is a regular one-dimensional integral around the singularity, which can be evaluated with a standard Gauss-Legendre quadrature. It is important to note, that the interpolation functions on the elements neighboring the pole must be at least C^0-continuous [6] at the collocation point.

III. REGULARIZATION OF NEARLY STRONG SINGULAR INTEGRALS

Nearly singular integrals appear if one wants to evaluate the electric or magnetic field vectors at points close to the boundary of a body. On the other hand, nearly singular integrals arise from boundary integral equations, when parts of the boundary surface become close to one another, as in the case of thin shapes or shells (see Fig. 3). For example, the field evaluations inside the thin steel plates of TEAM workshop problem No. 13 require an extremely accurate

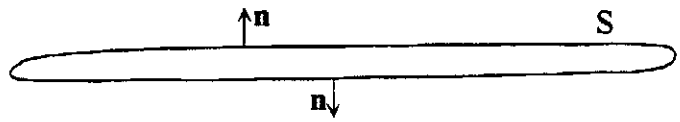

Fig. 3. Example of a thin body problem.

computation of nearly strong singular integrals [7]. Accurate evaluation of nearly singular integrals is a demanding task since the integrands vary rapidly on the surface of integrations when the source point is close to this surface. Now, we extend the approach of section II for the computation of nearly strong singular integrals.

Assuming that the observation point is close to the surface but not on the surface the kernel function (1) shows a nearly strong singularity. To transform the integral (2) into a nearly weakly singular integral and a one-dimensional integral around the singularity, we first find a 'projection point' P_1 of the observation point P (see Fig. 4) on the surface S.

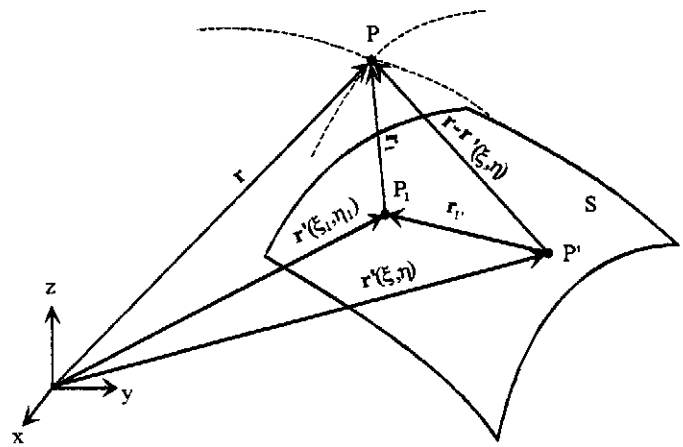

Fig. 4. 'projection point' P_1 of the observation point P on S and definition of vector $\mathbf{r}_1$ and vector $\mathbf{r}_{1'}$.

The 'projection point' P_1 should be located as near as possible to the observation point P and we assume now the point P_1 lies inside the boundary element S. The case that the image point is located on the border of element S can be treated similarly. The difference between the observation point P and the source point P' (see Fig. 4) can be written as

$$\mathbf{r}-\mathbf{r}'(\xi,\eta)=\mathbf{r}_1+\mathbf{r}_{1'}(\xi,\eta) \tag{19}$$

with the constant vector

$$\mathbf{r}_1=\mathbf{r}-\mathbf{r}'(\xi_1,\eta_1) \tag{20}$$

and

$$\mathbf{r}_{1'}(\xi,\eta)=\mathbf{r}'(\xi_1,\eta_1)-\mathbf{r}'(\xi,\eta) \tag{21}$$

where (ξ_1,η_1) are the coordinates of P_1 in the local parameter plane. Similar to (5), $\mathbf{r}-\mathbf{r}'$ is expanded in the neighborhood

of the point P_1 in a Taylor series in the local parameter plane and (22) can be easily obtained

$$\mathbf{r}-\mathbf{r}'=\mathbf{r}_1+\rho\,\mathbf{A}(\varphi)+0(\rho^2) \tag{22}$$

by the introduction of a polar coordinate system (3) centered at the point P_1 (ξ_1, η_1). Using (7) and (22) it is possible to obtain an asymptotic expression of the nearly singular kernel function (1), as follows

$$F(\rho,\varphi)\approx\frac{\mathbf{u}\cdot(\mathbf{r}_1+\rho\mathbf{A}(\varphi))\rho}{|\mathbf{r}_1+\rho\mathbf{A}(\varphi)|^3}N(\xi_1,\eta_1)J(\xi_1,\eta_1)\,. \tag{23}$$

Note, that

$$F(\rho,\varphi)-\frac{\mathbf{u}\cdot(\mathbf{r}_1+\rho\mathbf{A}(\varphi))\rho}{|\mathbf{r}_1+\rho\mathbf{A}(\varphi)|^3}N(\xi_1,\eta_1)J(\xi_1,\eta_1)=0 \tag{24}$$

if $\rho\to 0$. Adding and subtracting the asymptotic expression (23) in (2), we obtain

$$\begin{aligned}I=&\int_0^{2\pi}\int_0^{\rho_2(\varphi)}[F(\rho,\varphi)-\\&-\frac{\mathbf{u}\cdot(\mathbf{r}_1+\rho\mathbf{A}(\varphi))\rho}{|\mathbf{r}_1+\rho\mathbf{A}(\varphi)|^3}N(\xi_1,\eta_1)J(\xi_1,\eta_1)]d\rho\,d\varphi\\&+\int_0^{2\pi}\int_0^{\rho_2(\varphi)}\frac{\mathbf{u}\cdot(\mathbf{r}_1+\rho\mathbf{A}(\varphi))\rho}{|\mathbf{r}_1+\rho\mathbf{A}(\varphi)|^3}N(\xi_1,\eta_1)J(\xi_1,\eta_1)\,d\rho\,d\varphi\,.\end{aligned} \tag{25}$$

The integration of the second integral in (25)

$$G(\varphi)=\int_0^{\rho_2(\varphi)}\frac{\mathbf{u}\cdot(\mathbf{r}_1+\rho\mathbf{A}(\varphi))\rho}{|\mathbf{r}_1+\rho\mathbf{A}(\varphi)|^3}N(\xi_1,\eta_1)J(\xi_1,\eta_1)\,d\rho \tag{26}$$

with respect to ρ can be performed analytically (the dependence of φ has been omitted for the sake of brevity), as follows

$$\begin{aligned}G(\varphi)=&\left\{\mathbf{r}_1\cdot\mathbf{u}\left(\frac{4\sqrt{c}}{d}-\frac{2b\rho_2+4c}{d\sqrt{w}}\right)+\right.\\&+\mathbf{A}\cdot\mathbf{u}\left(\frac{(2b^2-4ac)\rho_2+2bc}{ad\sqrt{w}}-\frac{2b\sqrt{c}}{ad}\right)+\\&\left.+\frac{\mathbf{A}\cdot\mathbf{u}}{a\sqrt{a}}\ln\left|\frac{2\sqrt{aw}+2a\rho_2+b}{2\sqrt{ac}+b}\right|\right\}N(\xi_1,\eta_1)J(\xi_1,\eta_1)\end{aligned} \tag{27}$$

with

$$\begin{aligned}a(\varphi)&=\mathbf{A}\cdot\mathbf{A}\\b(\varphi)&=2\mathbf{r}_1\cdot\mathbf{A}\\c&=\mathbf{r}_1\cdot\mathbf{r}_1\\d(\varphi)&=4ac-b^2\\w(\varphi)&=a\rho_2^2+b\rho_2+c\,.\end{aligned} \tag{28}$$

Consequently, the final formula (29) for the calculation of nearly strong singular integrals can be obtained

$$\begin{aligned}I=&\int_0^{2\pi}\int_0^{\rho_2(\varphi)}[F(\rho,\varphi)-\\&-\frac{\mathbf{u}\cdot(\mathbf{r}_1+\rho\mathbf{A}(\varphi))\rho}{|\mathbf{r}_1+\rho\mathbf{A}(\varphi)|^3}N(\xi_1,\eta_1)J(\xi_1,\eta_1)]d\rho\,d\varphi\\&+\int_0^{2\pi}G(\varphi)\,d\varphi\,.\end{aligned} \tag{29}$$

Similar to (18), in (29) it can be seen that the first integral became a regular integral. The second integral is a regular one-dimensional integral, which can be evaluated with a standard Gauss quadrature. In the limit case ($\mathbf{r}_1\to 0$) equation (29) is identical to (18).

IV. NUMERICAL IMPLEMENTATION

For the numerical calculation it is comfortable to calculate the integrals in a local Cartesian system. The first integral in (18) is now a weakly singular integral. This weak singularity is removed by using polar coordinates (polar Gauss method) for the computation of the Gaussian points and of weight coefficients.

Thereupon, these coordinates of the points are transformed into the Cartesian coordinates and can thus be inserted in the Cartesian kernel function without any modification necessary. For a detailed derivation see [7]. Consequently, the final formula (18) can be transformed into Cartesian coordinates, as follows

$$\begin{aligned}I=&\sum_m\int_{\Gamma_m}\left\{\frac{\mathbf{u}\cdot(\mathbf{r}-\mathbf{r}'(\xi,\eta))}{|\mathbf{r}-\mathbf{r}'(\xi,\eta)|^3}N(\xi,\eta)\,J(\xi,\eta)-\right.\\&\left.-\frac{\mathbf{u}\cdot\mathbf{A}(\xi,\eta)}{\rho\,A(\xi,\eta)^3}N(\xi_1,\eta_1)\,J(\xi_1,\eta_1)\right\}d\xi\,d\eta+\\&+\sum_m\int_{\varphi_{1m}}^{\varphi_{2m}}\frac{\mathbf{u}\cdot\mathbf{A}(\varphi)}{A(\varphi)^3}N(\xi_1,\eta_1)\,J(\xi_1,\eta_1)\ln|\rho_{2m}(\varphi)A(\varphi)|\,d\varphi\end{aligned} \tag{30}$$

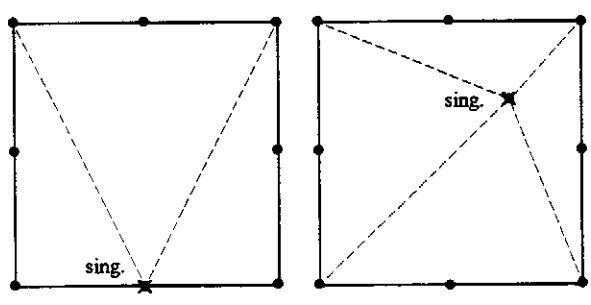

(a) (b)

Fig. 5. Subdivision of the transformed domain into elementary triangles, if the singular point is identical with the middle side node (a) and if the singular point lies inside the boundary element (b).

with

$$\rho \mathbf{A}(\xi,\eta)=\left.\frac{\partial \mathbf{r}'(\xi,\eta)}{\partial \xi}\right|_{\xi_1,\eta_1}(\xi_1-\xi)+\left.\frac{\partial \mathbf{r}'(\xi,\eta)}{\partial \eta}\right|_{\xi_1,\eta_1}(\eta_1-\eta). \qquad (31)$$

These modified Gaussian points are used to calculate the first weakly singular integral of (19). Equation (29) can be transformed into a similar one. It is important to note that according to the position of the observation point inside the element, the intrinsic domains of integration should be subdivided into a set of elementary triangles (see Fig. 5) in order to achieve a fast convergence.

V. NUMERICAL EXAMPLE

Some tests have been performed on the present method for the calculation of the singular integral. In the first test the singular integral (32) of order $O(1/r^2)$ given in [6] is evaluated on different distorted boundary elements. The integration region is a square ($-1 \le x' \le +1$ and $-1 \le y' \le +1$) in the z = 0 plane. Without loss of generality the following integral is considered

$$I=\int_{-1}^{+1}\int_{-1}^{+1}\frac{1}{r^2}\frac{x-x'}{r}dx'\,dy'. \qquad (32)$$

The kernel in (32) shows all the relevant features of any strongly singular integral arising in BEM. All computations were performed in double-precision arithmetic and for all computations the modified Gaussian points described in section IV are used.

A. Computation of the Cauchy principal value integral

The integration domain is subdivided into a different number of eight-noded boundary elements (see Fig. 6 and Fig. 7). The coordinates of the singular point x in the first and second case are located at the node connected to all four elements. The singular point is located for all cases on the position $\mathbf{r} = (-0.3, 0.2, 0.0)^T$. Note, that two middle nodes in fourth case are shifted.

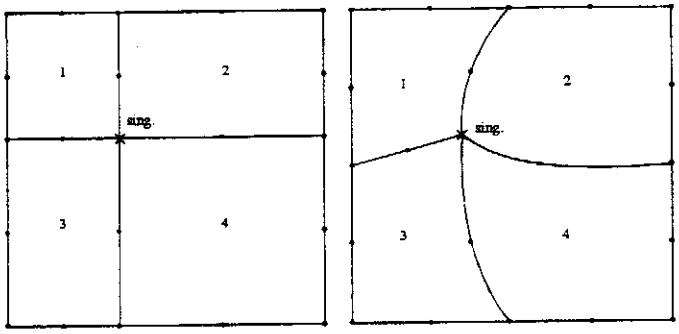

Fig. 6. Distorted meshes for testing the integration procedure (case 1 and case 2).

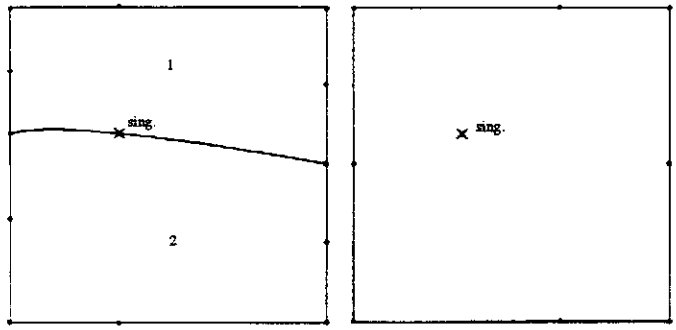

Fig. 7. Distorted meshes for testing the integration procedure (case 3 and case 4).

The quadratic integration domain is chosen for the purpose of comparisons since the integral (32) can be integrated in closed form. The number of Gaussian points for the one-dimensional line integral is identical to the number of points in the radial integration direction.

TABLE I

NUMERICAL RESULTS FOR THE CAUCHY PRINCIPAL VALUE INTEGRAL (32) (CASE 1 AND 2)

Gaussian points	case 1	case 2
3x3	-0.8785997736	-0.8707257728
6x6	-0.8790176221	-0.8790113071
8x8	-0.8790178921	-0.8790140361
analytically	-0.8790178909	-0.8790178909

TABLE II

NUMERICAL RESULTS FOR THE CAUCHY PRINCIPAL VALUE INTEGRAL (32) (CASE 3 AND 4)

Gaussian points	case 3	case 4
3x3	-0.8553715163	-0.8538898235
6x6	-0.8790648751	-0.8791044310
8x8	-0.8790071557	-0.8790179206
analytically	-0.8790178909	-0.8790178909

Table I and Table II give the numerical results obtained for the four cases shown in Fig. 6 and Fig. 7, compared with the analytically calculated value of the singular integral (32). Note, that using the standard product Gaussian quadrature without any regularization procedure no convergence to the correct solution can be achieved (about 300% error). The fast convergence in all four cases shows the effectiveness of the approach.

B. Computation of nearly singular integrals

The same mesh as in the fourth case is considered. Now the singular point is located above the element at the position $\mathbf{r} = (-0.3, 0.2, z)^T$. The z-coordinate is varied from 0.1 to 0.001.

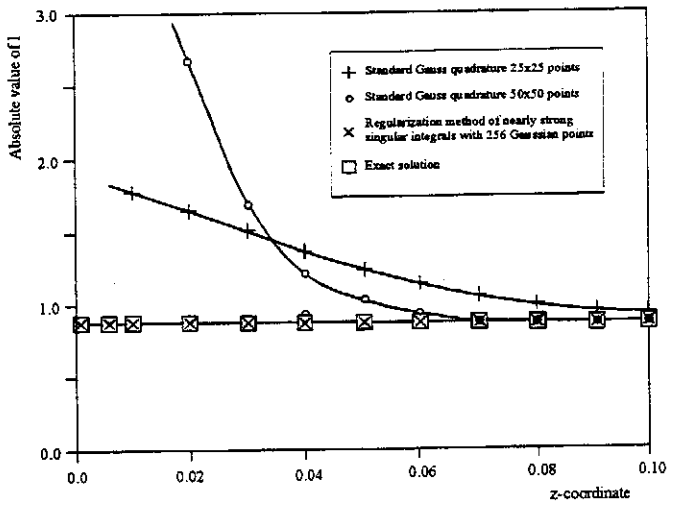

Fig. 8. Absolute value of integral (32) along the line x=-0.3 and y=0.2.

The value of the nearly singular integral (32) is plotted in Fig. 8 against the z-coordinate. If z = 0.0 the integral becomes a Cauchy principal value integral. It can be seen if the z-coordinate is lower than 0.06 the numerical computed integrals without any regularization but with a great number of Gaussian points became unstable. The nearly accurate value is always evaluated by the quadrature with the regularization procedure.

In Fig. 9 the relative error of the nearly singular integral (32) is shown for different Gaussian points and different numerical methods along the same line as used in Fig. 8.

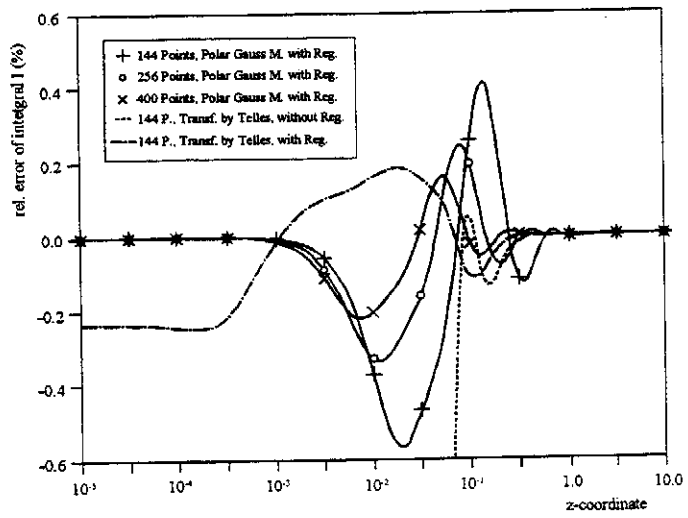

Fig. 9. Rel. error of integral (32) for different methods and Gaussian points.

The distance between the observation point and the element (z-coordinate) is varied from 10 to 10^{-5}. For comparison the error of the third order polynomial transformation method, proposed by Telles [8] is shown in Fig. 9. It can be seen that the error of the proposed regularization method is extremely low if the observation point lies nearly on the boundary, but the error is always lower than 0.6 %. The transformation method [8] without the proposed regularization works only for greater distances between the observation points and the boundary element. For greater distances even a better accuracy can be achieved by the combination of the polynomial transformation with the proposed regularization method.

VI. CONCLUSION

The method presented provides a very efficient procedure which can be easily implemented for the calculation of singular and nearly singular integrals on curved surfaces. The procedure has general validity. It can be applied to Cauchy principal value as well as to nearly strong singular integrals defined over curved surface elements of any type and order. Therefore, advanced BEM implementations (even with hierarchical shape functions) can now be developed easily for a larger class of problems.

REFERENCES

[1] K. Umashankar, A. Taflove, and S.M. Rao, "Electromagnetic scattering by arbitrary shaped three-dimensional lossy dielectric objects," *IEEE Trans. Antennas Propagat.*, vol. AP-34, pp. 758-765, June 1986

[2] J.R. Mautz, "A stable integral equation for electromagnetic scattering from homogeneous dielectric bodies," *IEEE Trans. Antennas Propagat.*, vol. 37, pp. 1070-1071, Aug. 1987

[3] M. S. Ingber and R.H. Ott, "An application of the boundary element method to the magnetic field integral equation," *IEEE Trans. Antennas Propagat.*, vol. 39, pp. 606-611, May 1991

[4] A. Glisson, "An integral equation for electromagnetic scattering from homogeneous dielectric bodies," *IEEE Trans. Antennas Propagat.*, vol. AP-32, pp. 173-175, Feb. 1984

[5] M. Guiggiani, P. Krishnasamy, T.J. Rudolphi, F.J. Rizzo, "A General Algorithm for the Numerical Solution of Hypersingular Boundary Integral Equations," *Transactions of ASME*, vol. 59, pp. 604-614, September 1992

[6] M. Guiggiani, P. Gigante, "A general algorithm for multidimensional Cauchy principal value integrals in the Boundary Element Method," *Transactions of ASME*, vol. 57, pp. 906-915, December 1990

[7] C.J. Huber, W.M. Rucker, R. Hoschek and K.R. Richter, "A New Method for the Numerical Calculation of Cauchy Principal Value Integrals in BEM applied to Electromagnetics," *IEEE Transactions on Magnetics*, 1997, in press

[8] J.C.F. Telles, "A self-adaptive co-ordinate transformation for efficient numerical evaluation of general boundary element integrals," *Int. Journal for Numerical Methods in Engineering*, vol. 24, pp. 959-973, 1987

[9] W.M. Rucker, E. Schlemmer, K.R. Richter, "The Solution of 3D Multiple Scattering Problems Using the Boundary Element Method," IEEE Transactions on Magnetics, vol. 30, pp. 3132-3135, Sept. 1994